IOPscience iopscience.iop.org

Home Search Collections Journals About Contact us My IOPscience

Muon showers deep underground

This article has been downloaded from IOPscience. Please scroll down to see the full text article.

1969 J. Phys. A: Gen. Phys. 2 374

(http://iopscience.iop.org/0022-3689/2/3/017)

View the table of contents for this issue, or go to the journal homepage for more

Download details:
IP Address: 129.252.86.83
The article was downloaded on 31/05/2010 at 10:17

Please note that terms and conditions apply.

J. PHYS. A (GEN. PHYS.), 1969, SER. 2, VOL. 2. PRINTED IN GREAT BRITAIN

Muon showers deep underground†

L. G. PORTER‡ and R. O. STENERSON
University of Utah, Salt Lake City, Utah, U.S.A.
MS. received 16*th December* 1968

Abstract. Data gathered with the University of Utah neutrino detector during late spring and summer of 1967 were used to study penetrating muon showers. These downward-going events contained two or more nearly parallel muons incident in a range of zenith angles between 30° and 75° having penetrated from 1500 to 6000 hg cm^{-2} of rock overburden. Studies were made to determine the radial extent of the showers, the frequency of occurrences of showers of each multiplicity, and the degree of isotropy of the arrival directions of shower events was plotted in celestial coordinates, with the result that these shower events could be characterized by a radius of 6 to 10 m, a multiplicity spectrum which is a power law in multiplicity having an exponent between $-3{\cdot}4$ and $-4{\cdot}0$ and no observable anisotropy. These shower data, together with measurements of events containing a single penetrating muon, were used to derive an empirical shower density function that accounts for the energy and angular dependence of the events of multiplicity 1, 2 and 3, as well as the absolute numbers of these events observed.

1. Introduction

The University of Utah neutrino detector, located under rugged overburden of the Wasatch mountain front, was used to study showers of high-energy (0·5–5 TeV) cosmic ray muons which penetrate to great depths underground, with the aim of developing an accurate empirical technique to describe measurements made at these depths. Muons with these energies are negligibly affected by the Earth's magnetic field, and their directions reflect the directions of their parent particles, which, because of their high energies, are most likely produced in the first few interactions of the nuclear-active cascade high in the atmosphere. Observations of the multiplicity, radial density distribution and frequency of energetic muons in air showers, then, provide almost direct information about the energy spectrum and nature of the muon parents and about the high-energy interactions which produced them; thus features of the empirical description of muon showers observed are directly related to those of the theoretical description of the primary interaction process that gives rise to these events.

Although more data were collected in this experiment than were previously available from the total of all other experiments performed at great depths underground (Barrett *et al.* 1952, Creed *et al.* 1965), the statistics at particular depths and zenith angles are sufficiently poor that interpretation and analysis of these events must necessarily involve *a priori* assumptions about the general character of the showers, which are then tested for consistency with the data. Agreement between the empirical representations obtained in this way and the data were optimized by iterative fitting procedures which demonstrated, at the same time, the sensitivity of these representations to variations of their parameters. It is hoped that these results will stimulate detailed theoretical studies of the energetic processes responsible for muon showers observed underground.

2. Apparatus

2.1. *Location and overburden of rock*

The University of Utah neutrino detector is located in an underground chamber excavated in the Silver King Mine near Park City, Utah. The chamber lies 1850 feet vertically below the surface of a mountain and three miles into the mountain by way of a

† Research supported by the National Science Foundation (U.S.A.).
‡ Now at Physics Department, Cornell University, Ithaca, New York, U.S.A.

horizontal railway through the Spiro tunnel. The geographic coordinates of the site are 40·623 °N latitude, 111·537 °W longitude, at an elevation of 6950 feet above sea level.

The amount of rock traversed by muons arriving at the detector from various directions was determined graphically; topographic maps from the U.S. Geological Survey with 40-ft contour intervals were used to draw profiles of the mountains as seen in vertical cross sections taken through the detector station at various azimuthal angles (Larson 1968). These are said to be reliable to ± 5 feet, making estimates of slant depth accurate to ± 20 feet.

Values for the average Z^2/A and the mean density of the rock surrounding our detector were determined from weighted averages using stratigraphic data and typical densities and chemical compositions of the various rock formations and deposits. At present, the best estimate for the mean rock density is 2·61 g cm^{-2}. Taking into account the porosity and probable water saturated condition of the rock, the average value for Z^2/A is 5·65.

2.2. *The detector system*

The complete kiloton detector shown in figure 1 consists basically of four directional Čerenkov counters, an array of 600 cylindrical spark counters, two large 16 kG solid iron

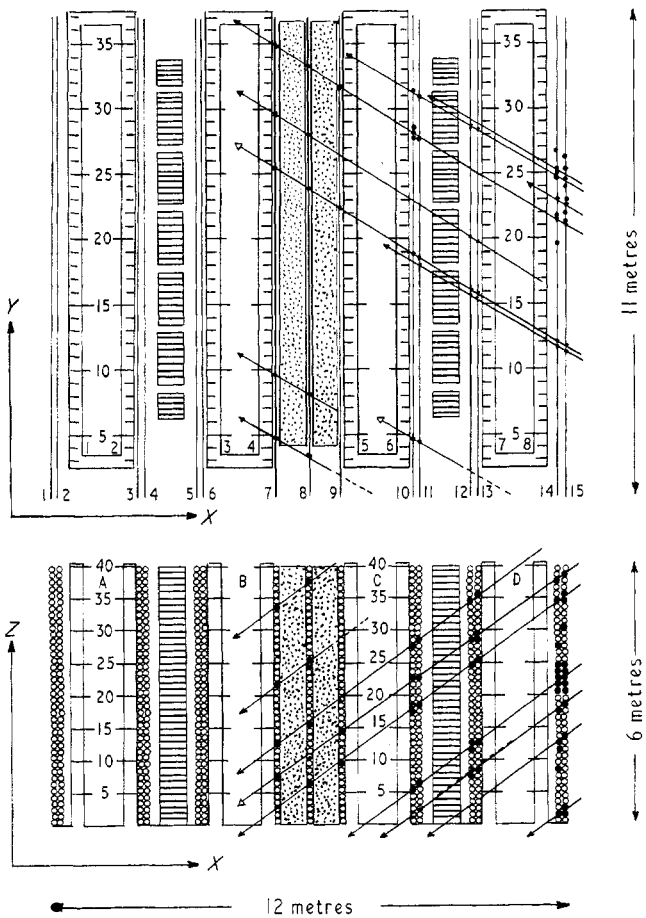

Figure 1. Front (XZ plane) and top (XY plane) views of the University of Utah neutrino detector. In the front view, the cylindrical spark counters are seen end-on as circles stacked in columns 40 high on either side of the water-filled Čerenkov counter tanks labelled A, B, C and D. The horizontally striped areas between A and B and between C and D are the solid iron magnets. The dotted areas between B and C are concrete. In the top view, columns of cylindrical spark counters appear as lines labelled 1 to 15, and light collecting walls of the Čerenkov tank are labelled 1 to 8.

electromagnets, and a complex electronic data gathering and digitizing system. When the passage of a particle or particles through the detector is indicated by the generation of a 'trigger' pulse by the Čerenkov counters, the cylindrical spark counters and data gathering electronics were activated. The localized nature of the discharges in the cylindrical spark counters made it possible to detect several discharges in a single cylindrical spark counter, an especially important feature in detecting large muon showers. The sparks in each cylindrical spark counter are located along the axis of the counter by a sonic ranging technique to a precision of about 3 mm, making it possible to reconstruct the trajectories of individual muons traversing the detector from the knowledge of the position of these sparks in the cylindrical spark counters. The *modus operandi* and details of this system as developed in a prototype detector have been reported previously in a series of three papers (Hilton *et al.* 1967, Keuffel and Parker 1967, Bergeson and Wolfson 1967).

A detailed investigation of detector dead time was made with the conclusion that it represented only about 1·6% of the total running time (Martin 1968). At the time the data for this work were collected, only Čerenkov tanks C and D, the magnet between them, and the nine columns furthest right of cylindrical spark counters were operational.

2.3. *The Čerenkov trigger efficiency*

Checks on systematic variations of the triggering efficiency were made by examining the rates recorded from run to run (Porter 1968). The overall rate of class A multiple muon events (see § 3) in each run was computed and plotted. Several runs (identified here as low triggering efficiency runs) had significantly lower rates than the majority of others (the high triggering efficiency runs) because of rapid growth of organic material in Čerenkov tanks during those runs.

The efficiency of each individual Čerenkov counter light collecting wall was determined during several special runs at high triggering efficiency. For these runs, tank B was temporarily put into operation; the system was triggered on coincident 'wall pulses' from tanks B and C when the efficiency of tank D was being measured, and on pulses from tanks B and D when the efficiency of tank C was being measured. Within the statistical accuracy (5%) of the measurements, each of the walls tested produced a 'wall pulse' in 86% of the events where a muon passed through the wall in the proper direction and was no closer than one foot to any edge of the wall (Martin 1968). This result was independent of the zenith or azimuth angle of the triggering muon; however, only muons with zenith angles greater than 45° could satisfy the conditions needed in these tests, and the individual wall efficiency at smaller zenith angles must be assumed to be the same as that at the larger angles.

2.4. *Digital cylindrical spark counter efficiency*

The efficiency of the cylindrical spark counters was measured in terms of individual column efficiencies by measuring the fraction of the time that an appropriate discharge appeared in the column when a muon passed through it; the muon trajectories were determined by discharges in other cylindrical spark counter columns (Larson 1968).

The efficiency of finding muon pairs where one of the muons passes through only one cylindrical spark counter group is not likely to be much greater than 72%. (Group I consisted of columns 7, 8 and 9; group II of columns 10 and 11; group III of columns 12 and 13; group IV of columns 14 and 15.) But the requirement that each of at least two triggering muons passes through at least two cylindrical spark counter groups increases the probability of their detection to 95% in the worst case. Events with higher muon multiplicities would, of course, be even less likely to be missed because of cylindrical spark counter failures.

3. Data gathering

Data tapes were obtained during the period from 19th May to 21st August 1967. The basic scanning programme used searched the tapes for single muon events. After looking visually at a large sample of plotted events of all types, it was decided that this

basic scanning programme (Bergeson *et al.* 1967), with slight modification, could be used to select the events most likely to be multiple muon events (Porter 1968), and these events could then be plotted up on a larger scale by hand and examined by eye.

From the more than 10 000 computer plots generated by the modified scanning programme which were visually scanned, 4095 were selected to be hand plotted at a larger scale because they showed definite evidence of the presence of more than one muon in the event.

The muons in the events on the plots were accepted to be recorded in six categories, according to which of the fiducial planes (figure 1) defining the aperture they passed through: (i) both forward walls of the Čerenkov tanks; (ii) the first forward Čerenkov wall (walls 6 and 7 for east- and west-going muons respectively) and at least two cylindrical spark counter groups; (iii) the second forward Čerenkov wall (walls 8 and 5 for east- and west-going muons respectively) and at least two cylindrical spark counter groups; (iv) the first forward Čerenkov wall and one cylindrical spark counter group; (v) the second forward Čerenkov wall and one cylindrical spark counter group; and (vi) neither forward Čerenkov wall, but striking some cylindrical spark counters in the detector in such a way as to indicate their presence as distinct and probably parallel particles. Information about the event on each plot was then punched onto computer data cards.

Events in which at least two muons each passed through at least two cylindrical spark counter groups and together could have triggered the detector independently of any other muons were recorded as class A; all others were relegated to class B. The 'triggering' muons which passed through two cylindrical spark counter groups in class A events had well-defined tracks in the detector and passed through a well-defined aperture; their parallelism could be firmly established to within a few degrees. Thus, only events in class A from high triggering efficiency runs were used in radial shower density measurement and the density spectrum calculations. The breakdown of these events on large plots into categories is shown in table 1.

Table 1. Breakdown of events on the large plots

Event description	Number of events	Disposition of data from plots
one Čerenkov wall not struck within prescribed limits	516	rejected
zenith angle too small or magnitude of azimuth angle in detector too large ($> 65°$)	256	rejected
no muons parallel to within 5°	18	rejected
projected zenith $> 20°$ zenith $< 30°$	474	punched on cards
class A events from high-efficiency runs	1391	punched on cards
class B events from high-efficiency runs	774	punched on cards
class A events from low-efficiency runs	420	punched on cards
class B events from low-efficiency runs	246	punched on cards

The efficiency of the modified scanning programme was checked by a visual scan of 1000 computer plots made of consecutively recorded events with more than four discharges. The fraction of class A muon pair events missed was found to be consistent with the estimates made on the basis of the measured cylindrical spark counter column efficiencies.

To check the visual scanning efficiency, the computer plots generated by the modified scanning programme selection for six data tapes were visually scanned at different times by two different persons. The first visual scanning of the computer plots was about 99% efficient in finding the plotted class A muon pairs, and about 96% efficient in finding the plotted class B muon pairs. None of the inefficiencies discussed seemed to be correlated with zenith angle, but statistics are poor and a more precise determination of this must await the collection of many more data.

4. Data analysis and results

4.1. *Compilation of data*

Multiple muon events analysed were distributed in two 18×26 matrices composed of these bins, one for westward-going and one for eastward-going muons. The eighteen 2·5° zenith intervals extended from 30° to 75°, and the twenty-six 5° azimuth intervals extended from $-65°$ to $+65°$ with respect to the detector x axis (figure 1). Each bin was associated with an effective depth $\bar{h}$ calculated by weighting the depths over the bin according to a vertical depth–intensity curve determined from a world-wide survey (Larson 1968). The distribution of class A events from high triggering efficiency runs in 10° zenith angle bins and 500 hg cm^{-2} depth bins is shown in table 2.

Table 2. Distribution of class A events in zenith angle and depth ranges

Zenith (deg)	Depth range (hg cm^{-2})	Multiplicity 1†	2	3	4	>4
30–40	1400–1900	260†	232	56	16	16
	1900–2400	472†	118	19	12	7
	2400–2900	95†	23	9	2	2
40–50	1400–1900	18	27	3	4	0
	1900–2400	1831	153	40	5	9
	2400–2900	2465	157	35	10	10
	2900–3400	281	14	0	1	1
50–60	1900–2400	48	14	0	0	0
	2400–2900	2315	107	17	4	6
	2900–3400	1756	86	12	3	0
	3400–3900	629	31	2	3	0
	3900–4400	39	2	1	0	0
60–70	2400–2900	19	1	0	0	0
	2900–3400	834	25	3	1	1
	3400–3900	1074	32	9	0	0
	3900–4400	471	18	2	0	0
	4400–4900	215	11	0	1	0
	4900–5400	35	4	0	0	0
	5400–5900	21	0	0	0	0
70–75	3900–4400	99	1	0	1	0
	4400–4900	138	4	1	0	0
	4900–5400	107	3	0	0	0
	5400–5900	25	1	0	0	0
	5900–6400	9	0	0	0	0
	6400–6900	11	1	0	0	0

† Single muons were not counted at zenith angles less than 35°. In addition, all single muon events were required to pass through three cylindrical spark counter groups, whereas muons from multiple events were required to pass through at least two cylindrical spark counter groups.

Measured live time for the high triggering efficiency runs corrected for the detector dead time (see § 2) was $2{\cdot}096 \times 10^6$ seconds. For the low triggering efficiency runs, the live time was measured to be $7{\cdot}90 \times 10^5$ seconds.

4.2. *Parallelism of particles in penetrating showers*

The parallelism of the penetrating particles observed in the detector is of interest because it carries implications about the points of origin of the showers. It is important

to determine whether the muon showers originate in interactions in the rock above the detector, or whether they are indeed a part of extensive air showers and come from very energetic cosmic ray interactions high in the atmosphere.

The angular resolution for single muons analysed by the computer was estimated to be 1° in projected zenith and better than 0·5° in azimuth (Bergeson *et al.* 1967). Aside from expected statistical fluctuations, no asymmetry with respect to converging and diverging pairs was observed. More than $\frac{2}{3}$ of the pairs are parallel to within 1° and, because of the mass of the detector, are known to have energies greater than 2 GeV. Coulomb scattering would be expected to produce differences of as much as a half degree between the projected angles of some pairs, even if they had been perfectly parallel at the surface of the Earth. The finite angular resolution of the detector would also tend to spread out the distribution. The most frequently observed spatial separation between pairs in the detector is about 4 metres. If the showers are produced in the rock, the points of origin must be more than 200 metres from the detector in order to account for the observed parallelism. Muons with this range must have energies of about 150 GeV. Pions of this energy produced in interactions in dense material have almost no possibility of decaying into muons before they interact; and, thus, ordinary showers originating in condensed matter are unlikely to produce particles with ranges of hundreds of metres. The cross section for pair production of muons of this energy by energetic muons is far too small to account for the observed number of multiple muons. Thus it appears that the only tenable conclusion is that almost all the multiple muon events originate in air showers.

4.3. *Arrival directions of showers in celestial coordinates*

The time and the zenith and azimuth angles of the muon trajectories recorded for each event were used to compute the arrival directions in terms of right ascension and declination of all class A and class B events containing two or more muons. Events were divided into separate data runs, and from each run only those events which occurred consecutively in time intervals of 24 siderial hours were plotted on a scatter plot.

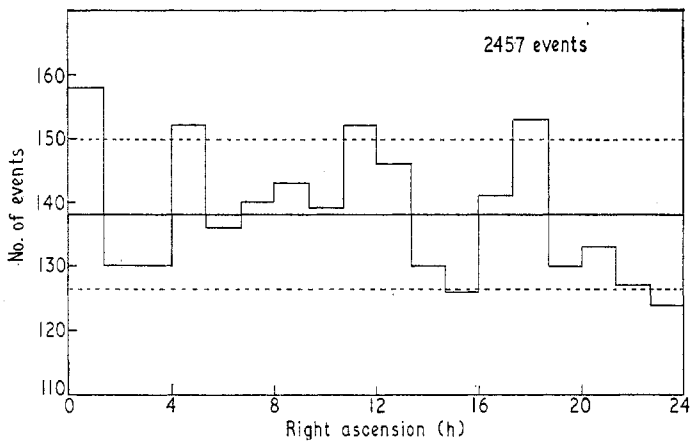

Figure 2. Distribution in right ascension of the directions of showers containing two or more high-energy muons.

In 24 siderial hours, a given angular bin in the detector scans the entire range of right ascension in every declination band; so, regardless of triggering efficiency, aperture or depth variations, the distribution in right ascension should be isotropic if the flux of showers is isotropic. High- and low-efficiency runs were first plotted separately as a check for any effect of triggering efficiency on the distribution. No systematic effect was found, and all runs were combined on one plot with 2457 events. Bands of declination from 10 °S to 80 °N were scanned for signs of a statistically significant clustering or dearth of points in a given right ascension interval. None were observed, but statistics were poor. Data from all declinations were combined, and the distribution in right ascension was plotted in 20° intervals in figure 2. No statistically significant anisotropy was found. The

1023 events with more than two muons in this sample were plotted separately on a similar plot with the same result.

It is estimated that these underground muon showers were produced by interactions of cosmic ray primaries having energies in the range 10^{14}–10^{15} ev. Surface air shower data (Chatterjee *et al.* 1965) have already established the isotropy of the primary flux in this energy range with more certainty than the statistics in our experiment afford; but the possibility that showers containing several muons might belong to a special class of muon-rich air showers produced chiefly by heavy nuclei made this study of interest. It is still possible that relatively rare high-multiplicity showers produced by heavy primaries might not have this isotropic distribution, but much more observational data would be needed to test this possibility.

4.4. *Spatial correlation between pairs of muons and the frequency spectrum of showers*

Although the area of the detector in the present experiment is large compared with other cosmic ray detectors operating underground, it is still small compared with the total area covered by most muon showers at great depths. Consequently, shower axes could not be located unambiguously. This fact precluded a direct study of the radial density distribution of muons in the showers. However, a study of the number of muon pairs against spatial separation (a decoherence curve) can yield some information about the radial extent of the showers. As pointed out by Barrett *et al.* (1952), if muon pairs are detected by observing coincidences between two small detectors of areas A_1 and A_2 separated by a distance x, then the number of coincidences expected is

$$C_{12}(x) = A_1 A_2 \sum_{M=1}^{\infty} M(M-1)F(M) \int \phi(M, r_1)\phi(M, r_2)\, \mathrm{d}a$$

where $F(M)$ is the number of showers of M muons with axes striking a small area da at distances r_1 and r_2 from the detectors A_1 and A_2, and $A\phi(M, r)$ is the probability that a given muon in a shower of M muons falls in an area A at a distance r from the axis. The integral is taken over the plane in which the detectors lie and can be done in closed form for the cases of a square and Gaussian muon radial density distribution with characteristic radius σ. In either case, we will represent the integral by $G(x, \sigma)/\pi\sigma^2$. In the square distribution

$$G(x, \sigma) = 1 - \frac{2}{\pi}\sin^{-1}\left(\frac{x}{2\sigma}\right) - \frac{x(4\sigma^2 - x^2)^{1/2}}{2\pi\sigma^2}$$

and for the Gaussian distribution

$$G(x, \sigma) = \exp\left(\frac{-x^2}{2\sigma^2}\right).$$

Some special problems were associated with making this type of study with a single large-area detector having sensitive areas which are strongly dependent on zenith and azimuth. The approach taken was to subdivide some of the sensitive areas in each angular bin into smaller areas, each of which had an area of less than 0·1 m^2. The subdivided areas were all chosen so that a muon passing through them would traverse at least two groups of cylindrical spark counters and at least one forward Čerenkov wall. These areas were so small that the likelihood of seeing a pair in any one of them individually was very small. (Less than 0·5 % of the pairs had separations of less than 0·3 m.) The product of the areas of each pair of small areas was formed for all pairs which, if simultaneously struck, would result in a trigger for the detector. A sum of these products for pairs of areas in each separation interval was designated as $A_1A_2(I, J, K)$. Then the number of pairs observed in the Ith zenith angle bin, the Jth azimuth bin and the Kth separation interval should be given for the present detector by

$$C_{12}(K-1 < x < K) = \epsilon(I, J)\frac{A_1A_2(I, J, K)}{\pi\sigma^2} \sum_{M=1}^{\infty} M(M-1)F(M)G(\bar{x}, \sigma)$$

where the midpoint of the separation interval is $\bar{x} = \frac{1}{2}(2K-1)$; σ is the assumed shower radius and $\epsilon(I, J)$ is the computed average triggering efficiency for the class A events

from which the pairs were selected. The efficiency for triggering an individual event is given in terms of the Čerenkov wall inefficiencies and the numbers of muons n_1 and n_2 which pass through the first and second forward Čerenkov walls respectively as

$$E = \{1-(0{\cdot}14)^{n_1}\}\{1-(0{\cdot}14)^{n_2}\}.$$

To improve statistics, the data and the predicted numbers were put into 10° zenith angle bins and 500 hg cm^{-2} depth bins. A χ^2 calculation for the fit of the predicted numbers to the observed numbers in the separation intervals was then made in each of these large

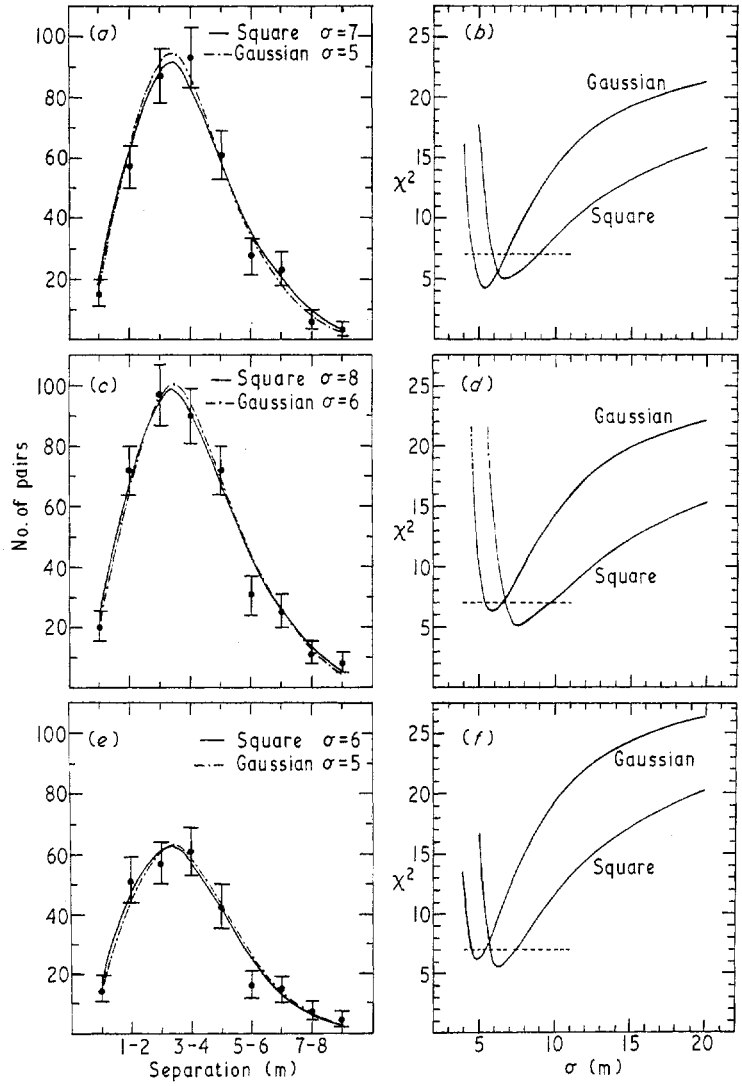

Figure 3. The measured numbers of pairs as a function of separation together with the predictions based on a square and a Gaussian radial distribution. In the plots of χ^2 against shower radius, the dotted line delineates the range of σ at the 33% confidence level.

bins for integral values of σ from 5 to 20 metres. The sum $\Sigma_{M=1}^{\infty} M(M-1)F(M)$ was determined in each case by finding the minimum χ^2 for each value of σ. The 0–1 m and the 9–10 m intervals were not used in making these fits.

The results of these calculations are shown in figure 3 for 1063 pairs for zenith angles and depths in the ranges 40 to 60 degrees and 1900 to 2400 hg cm^{-2}, respectively, using a

square and a Gaussian radial distribution. The observed number of pairs are plotted with their statistical flags. A curve is drawn through the points predicted by the best fit to the data, and a plot of χ^2 against σ is also provided in each plot. The minimum value of χ^2, when $G(\bar{x}, \sigma)$ was made a constant, was always in excess of 20, which indicates that there was sensitivity to the function $G(\bar{x}, \sigma)$ and the fits were not entirely determined by the $A_1A_2(I, J, K)$ factors which reflect the geometry of the detector. The broad minimum in χ^2 may reflect the fact that all showers, even at a given depth, do not have the same radius. In our case, it was necessary to combine the bins at several depths and zenith angles, and there was considerable coarseness in our calculations; so it is felt that only a reasonable estimate for the range of σ can be obtained from our results. If the range of values for σ which gives χ^2 values less than 7 (the 33% confidence level) is taken, then the range is 6 to 10 metres. The fit to the Gaussian and the square radial distribution appear to be equally good.

An estimate of the mean number of muons in the shower was also obtained from these results. Note that

$$\sum_{M=1}^{\infty} M(M-1)F(M) = I_0\langle M(M-1)\rangle$$

where I_0 is the total number of showers per unit area and $\langle M(M-1)\rangle$ is the average value of $M(M-1)$. The expression for the number of single muons $N_s(I, J)$ expected to trigger the detector in a given angular bin (I, J) gives

$$\frac{N_s(I, J)}{\eta A(I, J)} = \sum_{M=1}^{\infty} MF(M) = I_0'\langle M\rangle$$

where $A(I, J)$ is the aperture area for single muons and η is the single muon triggering efficiency. The sums over $N_s(I, J)$ and $A(I, J)$ were taken over 10° zenith bins and 500 hg cm^{-2} bins. Again the possible zenith and depth variations of $F(M)$ were ignored, as only an average value of M is sought in each bin. Using these results and the results from the analysis of pair separations, one obtains

$$\frac{I_0\langle M(M-1)\rangle}{I_0'\langle M\rangle}\frac{T_s}{T_p} = \frac{\langle M^2\rangle}{\langle M\rangle} - 1$$

(where T_s/T_p corrects for the small difference in running times during which the 'singles'

Table 3. Shower radii and multiplicity

Zenith range (deg)	Depth range (hg cm^{-2})	$\sigma_+, \sigma_0, \sigma_-$ (m)	$\frac{\langle M^2\rangle}{\langle M\rangle}$	δ
40–50	1900–2400	10	2·11	3·40
		7	1·52	3·70
		6	1·41	3·90
40–50	2400–2900	11	2·10	3·40
		8	1·70	3·60
		7	1·58	3·70
50–60	2400–2900	8	1·56	3·70
		6	1·37	3·95
		6	1·37	3·95

and 'pairs' were observed). The values of $I_0\langle M(M-1)\rangle$ were computed corresponding to the range of σ which gave $\chi^2 < 7$. Since $1 < \langle M\rangle < \langle M^2\rangle^{1/2}$, one can infer the inequality $1{\cdot}37 < \langle M^2\rangle < 4{\cdot}4$ covering the three sets of results; thus, on the average, the muon showers deep underground have very few mesons. If the number distribution is assumed to be given by a power law $M^{-\delta}$, then the ratio $\langle M^2\rangle/\langle M\rangle$ can be used to determine δ. The results of these measurements on σ, $\langle M^2\rangle/\langle M\rangle$ and δ are tabulated in table 3.

Although the estimate of the shower radius obtained in the present experiment is somewhat smaller than that obtained for nearly vertical showers at 1600 hg cm^{-2} depth by Barrett *et al.* (1952), it does not appear to be so small as to be in conflict with the current ideas on pion production in the primary interaction. The measured values of δ are higher than those measured by Barrett *et al.* (1952). These higher values are highly suggestive of the contribution of a new process producing predominantly events containing small numbers of muons; but, unfortunately, the results are not precise enough in themselves for one to draw any firm conclusion.

4.5. *Density spectrum of underground muon showers*

The concept of a density spectrum has long been used in connection with the analysis of extensive air showers above the ground where particles are detected by arrays of Geiger–Muller counters or scintillators. The number of n-fold coincidences in such a detector array can be related through counter areas and Poisson statistics to the average densities of the showers striking the array. In this way, the differential density spectrum (number of showers per second per steradian having densities in the range Δ to $\Delta+\mathrm{d}\Delta$ at the detector location) can be estimated from experimental measurements and related through shower theory to other features of cosmic ray phenomenology.

In this section, an attempt to apply the same type of analysis to muon showers underground is made. This approach may be questioned because large differences exist between typical showers observed above ground and the showers of energetic muons observed underground. Showers above ground contain thousands of particles spread over large areas so that the variation in density of shower particles over an array of detectors with an area small compared with the shower area may be neglected. Muon showers underground at the depths involved in the present experiment contain on the average only a few particles which are distributed within a radius of 6 to 10 metres from the shower core. However, a muon shower radius of 6 to 10 metres implies that the showers cover an area of hundreds of square metres; this area is large compared with the detector area (in most bins, a factor of 5 or more), and the assumption that the muons are on the average uniformly distributed over this area may still not be unreasonable.

The deriving of a muon density spectrum from our observations may be defended even if the meaning of the result may not be so clearly interpreted as the density spectrum of the electromagnetic showers on the Earth's surface. It must be remembered that the function derived is essentially empirical and, in a sense, represents a means of describing what was observed in compact form; the complexity of the aperture for multiple muon events, the wide variations in depth with angle, and statistics made it desirable to try to find some explicit way of expressing our results in a form which folded out these special features of our detector and experiment. Of course, the measure of our success in doing this must come from the application of the result and the density spectrum concept to other experimental set-ups with good agreement. Even then, it may not be assumed that particular features of the empirical function have any special physical significance, for another functional form may conceivably give a spectrum of similar shape. A theoretical explanation of the spectrum shape may involve folding in the effects of many physical processes, but the existence of such an empirical spectrum for comparison with theoretical prediction is, in fact, necessary.

The number of muons detected underground is expected to be a function of the distribution of shower densities, zenith angle and depth. A trial differential density spectrum was assumed having the convenient form

$$n(h, \theta, \Delta)\,\mathrm{d}\Delta = G(h)F(\theta)H(\Delta)\,\mathrm{d}\Delta.$$

Each of the factors, of course, could be complicated and involve several parameters.

$H(\Delta)$ was taken to be of the form

$$H(\Delta) = \begin{matrix} K_\beta \Delta^{-\beta} \text{ for } \Delta > \Delta_0 \\ K_\alpha \Delta^{-\alpha} \text{ for } \Delta < \Delta_0 \end{matrix}$$

where $K_\alpha \Delta_0^{-\alpha} = K_\beta \Delta_0^{-\beta}$. This form is not an unreasonable one to take, because, in two experiments in which underground muons were correlated with the sizes of the concommitant air showers above ground (Barrett *et al.* 1952, Chatterjee *et al.* 1965), it was deduced that the number of underground muons was related to the size of the air shower by a power law. Since the size spectrum for air showers is approximately given by the power law in N, the density spectrum for underground muon showers is expected to be a power law in Δ, the muon density. When there is only one muon present within the shower radius σ, the density of showers is effectively cut off at $\Delta = 1/\pi\sigma^2$. What is more likely physically is that the exponent of the density spectrum should change at this density. In fact, a density spectrum with a single slope is a physical impossibility in that it would predict an infinite counting rate. Considerations of the computational problems involved in determining values for the parameters to fit the data were also involved in this choice for $H(\Delta)$, because a sharp break in the slope is not to be expected physically and many ways of producing a smoother change in the slope of the density spectrum with density might have been used.

The decision to try constructing a density function that could predict single muon intensities as well as rates for multiple muon events with this form for $n(h, \theta, \Delta)$ imposed a constraint on $G(h)$. In applying the density spectrum concept to predict the muon intensity at a fixed zenith in a detector of area S at a depth h, a definite integral over Δ is involved. The rate of events where n muons are observed will be

$$R = \epsilon(n) \int_\Omega \int_{\Delta=0}^{\infty} P_n(\Delta S) n(h, \theta, \Delta)\, \mathrm{d}\Delta\, \mathrm{d}\Omega$$

where $\epsilon(n)$ is the detector efficiency for n muons and $P_n(\Delta S) = \{(\Delta S)^n/n!\} \exp\{-(\Delta S)\}$ is the Poisson probability for observing n muons in a shower of density Δ. $G(h)$, then, must have the same dependence on h as the vertical depth–intensity curve which is reasonably well known. It was assumed that the integral energy spectrum for muons at sea level can be represented by a power law, $I(>E) \propto E^{-\gamma}$. An approximate energy–range relation (Barrett *et al.* 1952, Kobayakawa 1967) can then be used to predict the depth–intensity relation

$$I(h) \propto \frac{a'}{b} \{\exp(bh) - 1\}^{-\gamma}.$$

a'/b is a slowly varying function of E; but, over the range of energies for which the fit to the depth–intensity curve was to be made, it was assumed to be constant. b and γ actually both increase slightly with energy, but a good fit in the range 1000–6000 hg cm^{-2} can be obtained if b is fixed and only γ is allowed to increase with depth. The form for $G(h)$, which, by hypothesis is proportional to $I(h)$, then was taken as

$$G(h) = C\{\exp(bh) - 1\}^{-\gamma}$$

where $b = 3{\cdot}5 \times 10^{-4}$ hg^{-1} and $\gamma = 2{\cdot}4 + 0{\cdot}25 \ln(h/10^3 \text{ hg})$. The correct value of b is not certain, because the magnitude of the contribution of photonuclear interactions (and other possible energy loss mechanisms as yet unobserved; Bergeson *et al.* 1967, 1968) to this term is not definitely known. The value used here is the b, which, when used in Kobayakawa's range–energy calculations (Kobayakawa 1967), gives agreement to within 3% with his exact calculation using his estimate of $b(E)$. Setting C equal to $1{\cdot}55 \times 10^{-7}$ s^{-1} cm^{-2} sr^{-1} gives a fit (to within 10% from 1000 to 6000 hg cm^{-2}) to the world-wide depth–intensity curve given by Larson (1968), but in our calculations C will be included in the normalization factor K_β.

Several forms for $F(\theta)$ were tried in the fitting and these will be discussed later. It is important to note that, in choosing the values of b, γ and C in the strong energy-dependent factor $G(h)$ to agree with the measured vertical depth–intensity of cosmic ray muons, the sensitivity of the analysis to the exact value of the rock density is decreased by these choices, which act, to a certain extent, as scale factors.

The number of observed events of various multiplicities in each of the $2{\cdot}5 \times 5$ deg^2 angular bins was obtained by having the computer sort the class A events that had been punched on computer cards. The number of single muon events in each angular bin was known from the work of Bergeson *et al.* (1967). The trial density function was used to compute predicted values for the number of single, double and triple muon events in each bin. K_β, the normalization factor for all three calculations, was determined by demanding that the total predicted number of two muon events be exactly equal to the number observed. In doing these calculations with the trial density function, the correct value of $\bar{h}$ in each angular bin was substituted into $G(h)$. The apertures corresponding to the single muon measurements and, separately, to the multiple muon measurements were evaluated in each of the angular bins for this analysis.

For single muons, the detector aperture for a given angular bin can be defined by a single area A_s and the solid angle of the bin $d\Omega$. The projected areas of the two Čerenkov forward wall fiducial planes on a plane normal to the incident muon trajectory must overlap in some area in order for a single muon to trigger the detector, and that overlap area is the only sensitive area for single muons. A_s is further restricted by the requirement that single muons must pass through at least 3 cylindrical spark counter groups as well (Bergeson *et al.* 1967).

In the case of multiple muons, coincident wall pulses can be produced by muons striking other areas of the detector in the right combinations as long as both forward walls are struck by the muons in the event. In passing through the area of a forward wall, a muon may also pass through at least two, one, or none of the cylindrical spark counter fiducial planes, and definite effective areas for each of these possibilities are determined by the overlapping areas of the forward wall fiducial planes and the cylindrical spark counter fiducial planes as seen from the muon's point of view. So for multiple muon events, five sensitive areas were defined which correspond directly to the first five categories defined in § 3 for the muons in an event. The probability of observing muons in any category depends on the size of the associated sensitive area. A further complication is the fact that the triggering efficiency is dependent on the number of muons striking each forward wall. The details of the numerical evaluation of the rate integrals over shower density and detector solid angle are given in Porter's (1968) thesis. These integrals involve products of the Poisson probabilities of observing muons in the various combinations of sensitive areas and the differential density spectrum multiplied by the triggering efficiency for each combination of sensitive areas.

A sum over azimuth angles was performed for both the experimental numbers and the predicted numbers. This sum collected the two sets of numbers into 18 zenith angle bins from 30° to 75° corresponding to slant depths ranging from 1500 to 6000 hg cm^{-2}. A χ^2 for the fit of the predicted numbers to the data in these bins was then calculated for events of each multiplicity. In total, these fits were made to 13 267 single muon events, 1065 two muon events, and 209 events with three muons. There were, in addition, 63 events with four muons and 52 events having more than four muons. Plots of χ^2 against various values of the parameters were then made in an attempt to find a set of parameters which gave a good fit for all multiplicities.

The first trials were made setting $F(\theta) = 1$ (i.e. no zenith-angle dependence). The parameters varied were α, β and Δ_0. It was found that fairly good fits to the double and triple muon events could be made, but the single muon events could not be fitted as the predicted numbers were consistently low. The fractional discrepancy between the predicted and observed numbers increased slightly with zenith angle. By taking ratios of the observed numbers to predicted numbers at each zenith angle, it was determined that multiplying the predicted numbers by the factor $9/(4+5\cos\theta)$ in each zenith angle (θ) bin would bring the sets of numbers for 'singles' into better agreement. So $f(\theta)$ was set equal to this factor. The resulting fit was better for the single muon events, but the predicted numbers of 'doubles' and 'triples' were too high at the larger zenith angles. It was concluded that a simple multiplicative factor giving the zenith-angle dependence of our density spectrum would not be able to give a good fit for events of all multiplicities.

At this point, the behaviour of preliminary Monte Carlo calculations by Adcock, Wdowczyk and Wolfendale on extensive air shower development which gave integral muon density curves at 35° and 60° suggested that the point of discontinuity in the slope of the density factor could be a function of zenith angle. This had the desired effect of making the 'singles' more strongly affected by zenith angle than were the 'doubles' and 'triples'. Accordingly, a new trial differential density function was chosen of the form

$$n(h, \theta, \Delta)\,\mathrm{d}\Delta = G(h)H(\Delta, \theta)\,\mathrm{d}\Delta.$$

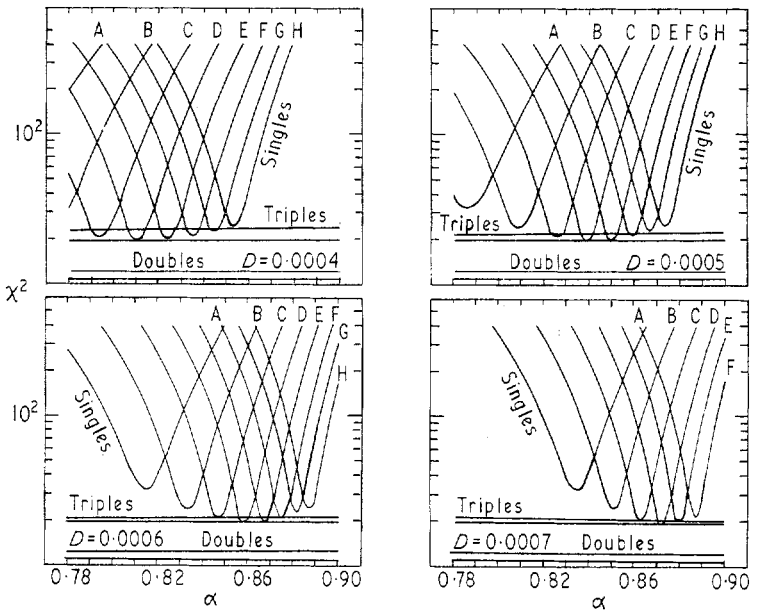

Figure 4. Plot of χ^2 against α for singles, doubles and triples, with β fixed at $-2{\cdot}75$. Curves correspond to values of $R = E/D$: A, $R = 1{\cdot}5$; B, $R = 2{\cdot}0$; C, $R = 2{\cdot}5$; D, $R = 3{\cdot}0$; E, $R = 3{\cdot}5$; F, $R = 4{\cdot}0$; G, $R = 4{\cdot}5$; H, $R = 5{\cdot}0$.

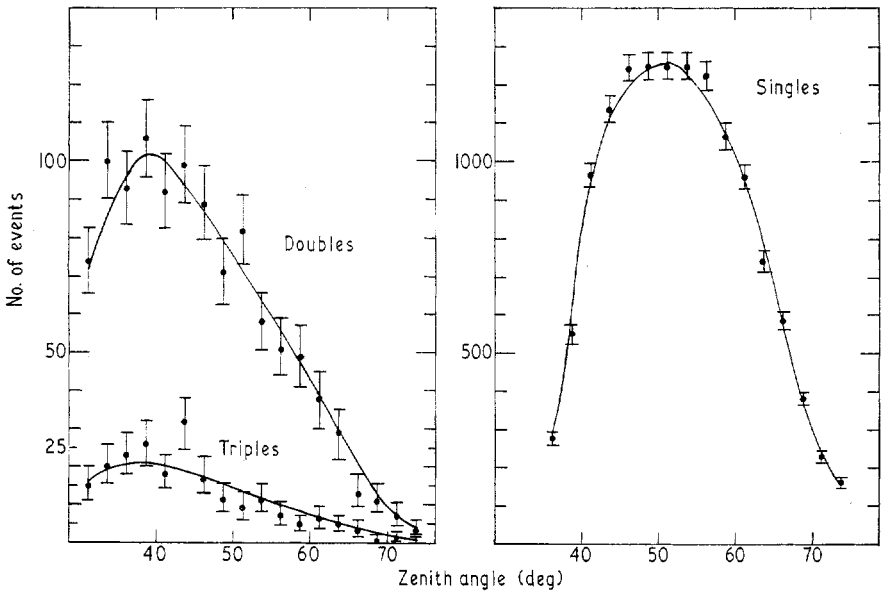

Figure 5. Measured angular dependence of singles, doubles and triples compared with the predictions of the empirical density spectrum.

$H(\Delta, \theta)$ has the same dependence on density that $H(\Delta)$ had previously, but the point of intersection of the two power laws in density is determined by $\Delta_0 = (D+E\cos\theta)\ \mathrm{m}^{-2}$, giving one more parameter to vary in making the fit.

Figure 4 shows plots of χ^2 against α for 'singles', 'doubles', and 'triples' with β fixed at $-2{\cdot}75$. In each plot, D has a different value; the various curves correspond to different values of $R = E/D$: A, $R = 1{\cdot}5$; B, $R = 2{\cdot}0$; C, $R = 2{\cdot}5$; D, $R = 3{\cdot}0$; E, $R = 3{\cdot}5$; F, $R = 4{\cdot}0$; G, $R = 4{\cdot}5$; H, $R = 5{\cdot}0$. The χ^2 for the 'doubles' and 'triples' remains fairly stationary (only the limits of the variation being shown in the figure), while the χ^2 values for the 'singles' reach minima at various α for different R values. The lowest χ^2 occurs for $R = 2{\cdot}5$ to $3{\cdot}0$ in all plots, however.

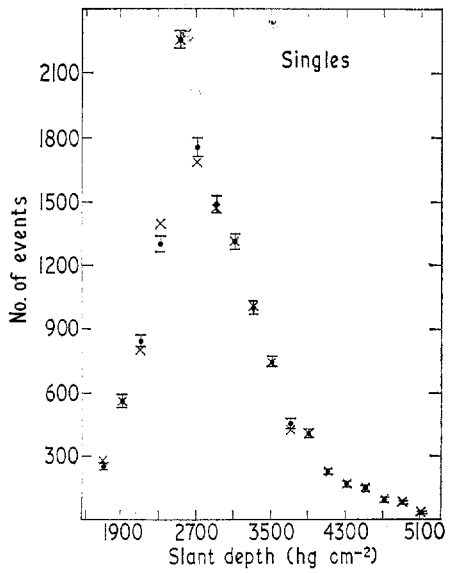

(*a*)

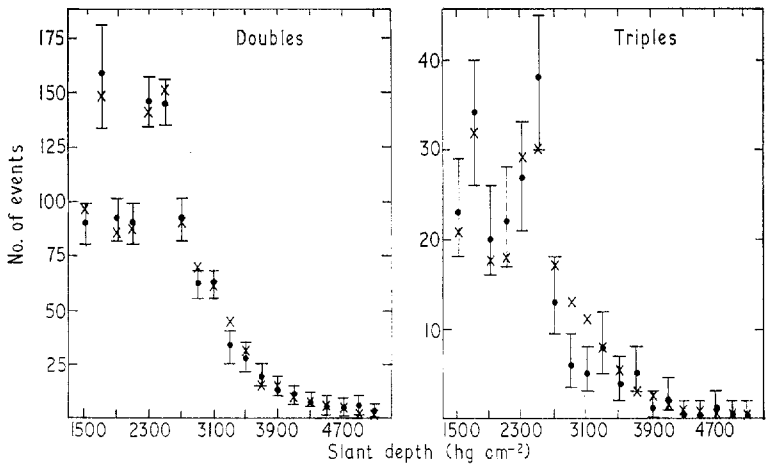

(*b*)

Figure 6. Measured depth dependence of singles, doubles and triples compared with the predictions of the empirical density spectrum.

The minima in the χ^2 curves in all the preceding figures are somewhat broad for the 'triples'; and, although the 'singles' fit is very sensitive to the value of α for the fixed β and R, there is not, among the best fits, any unique set of parameters that gives a significantly

better fit than some other. Thus it seemed unfruitful to proceed further with the fitting, since fits near the 30% confidence level could be obtained for the 'singles' and 'triples' and even better fits could be obtained for the 'doubles'. Several different sets of parameters which gave nearly equally good fits with our functional form are listed below.

	β	α	D (m^{-2})	E (m^{-2})	Normalization factor
(*a*)	2·75	1·8475	0·0006	0·0015	$192{\cdot}89 \times 10^{-8}$
(*b*)	2·86	1·8975	0·002	0·002	$130{\cdot}93 \times 10^{-8}$
(*c*)	3·2	1·9210	0·004	0·004	$35{\cdot}11 \times 10^{-8}$

Using the parameters in set (*a*) several additional checks were made of the predictions of the density function. This particular combination of parameters was chosen here because the fits for doubles and triples improve slightly as β decreases. Figure 5 is a plot of predicted numbers against observed numbers of events in each of the eighteen 2·5° zenith bins used in the χ^2 calculations. The observed numbers are shown with their statistical flags, and a curve is drawn through the numbers predicted by the density function, showing agreement with the angular dependence of the data. Figure 6 is a plot of predicted numbers against observed numbers in 200 hg cm^{-2} intervals. The angular dependence of the predicted numbers has been folded out using the density function. Statistical flags were put on the observed numbers represented by full circles and predicted numbers were drawn as crosses. The agreement here served as a check on the depth-dependent factor in the density spectrum.

As a further check on the predictions, the number of expected two muon events where both muons go through both forward walls was computed and compared with the observed number. The numbers are respectively 131·5 and 134. The predicted number of three muon events where all three muons go through both forward walls was 7·2, while the

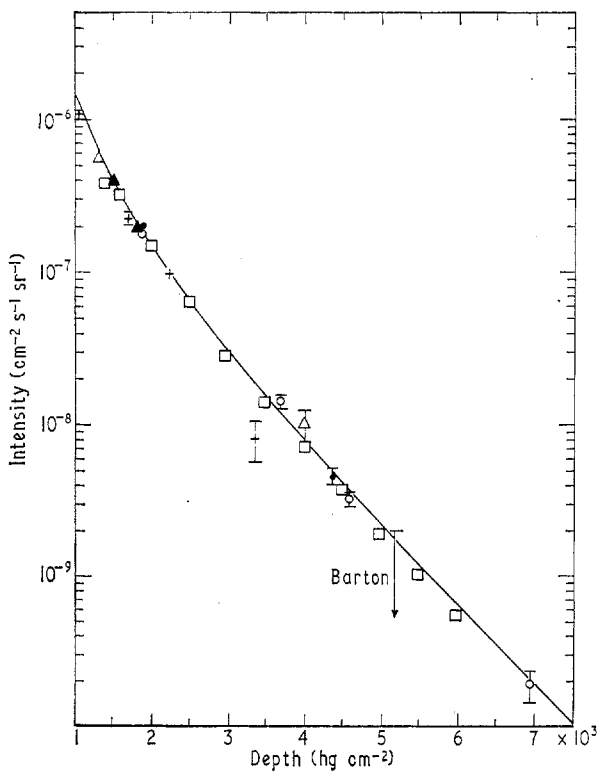

Figure 7. Vertical depth–intensity predicted by the empirical density spectrum. ● Archar *et al.* 1965; ○ Miyake *et al.* 1964; ▲ Bollinger 1952; △ Castagnoli *et al.* 1965; + Barton *et al.* 1968; ■ Barrett *et al.* 1952; □ predicted by density spectrum.

observed number was 4. The total number of four muon events where all four muons go through at least two cylindrical spark counter groups and none went through only one group was also predicted to be 38·2 and compared with the observed number, 35. The plots in the figures 5 and 6 and the above comparisons indicate that the density spectrum can be used to predict rates within statistics for events of various multiplicities in our detector.

Other experiments studying muon showers at great depths were done with detectors having a sensitivity that was greatest for vertical showers and areas that were about 1 m^2. Our empirical density spectrum was used to compute the expected vertical intensity of single muons as well as the vertical intensity of multiple events in 1 m^2 detectors at various depths. The results and comparisons with observations are shown in figure 7 and table 4 for the single and multiple events respectively. There is agreement within statistics and within the accuracy (10%) to which the depth–intensity curve is known.

Table 4. Comparison of intensities predicted by empirical density spectrum with other observations

Depth (hg cm^{-2})	Multiple muon intensities predicted by the empirical density spectrum ($cm^{-2}\,s^{-1}\,sr$)	Measurements by other groups Depth (hg cm^{-2})	Measurements ($cm^{-2}\,s^{-1}\,sr^{-1}$)
1500	$8{\cdot}16\times10^{-10}$	1574 (Barrett *et al.* 1952)	$6{\cdot}6^{+1{\cdot}2}_{-1{\cdot}0}\times10^{-10}$
2000	$3{\cdot}12\times10^{-10}$	1812 (Creed *et al.* 1965)	$7{\cdot}3^{+2{\cdot}9}_{-1{\cdot}9}\times10^{-10}$
2500	$1{\cdot}34\times10^{-10}$		
3000	$6{\cdot}17\times10^{-11}$		
3500	$2{\cdot}99\times10^{-11}$		
4000	$1{\cdot}50\times10^{-11}$	4100 (Creed *et al.* 1965)	$1{\cdot}0^{+2{\cdot}4}_{-0{\cdot}8}\times10^{-11}$
4500	$7{\cdot}77\times10^{-12}$		
5000	$4{\cdot}09\times10^{-12}$		
5500	$2{\cdot}19\times10^{-12}$		
6000	$1{\cdot}18\times10^{-12}$		

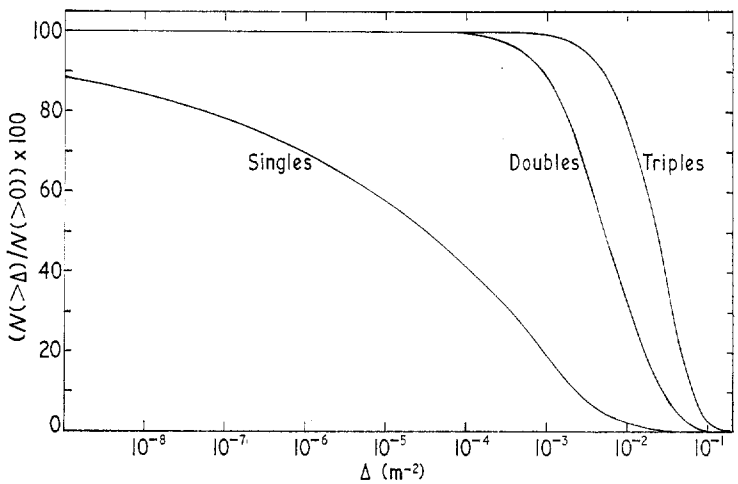

Figure 8. Percentage of singles, doubles and triples predicted for the present experiment by the empirical density spectrum that comes from showers of density greater than Δ.

To determine the range of shower densities sampled by the present experiment, a numerical integration was performed over limited ranges of density using the apertures for single and, separately, for multiple muon events and the estimates of $\bar{h}$ in each bin corresponding to the measurements made to see what fraction of the predicted events of each multiplicity came out of each range of density. These results are shown in figure 8. The calculation for the single muon samples the broadest range of densities, there being 10% of the single muons produced by shower densities less than 10^{-9} m^{-2}. Events of higher multiplicity sample successively higher regions of density, the response of the calculation becoming a sharper function of density as the multiplicity of the event increases. The maximum shower density sampled was 10^{-1} m^{-2}, which limits our knowledge of the shower density function in the high-density region. Thus, with more data at higher multiplicities, one might hope to determine β more precisely and also narrow down the range of values for the other parameters.

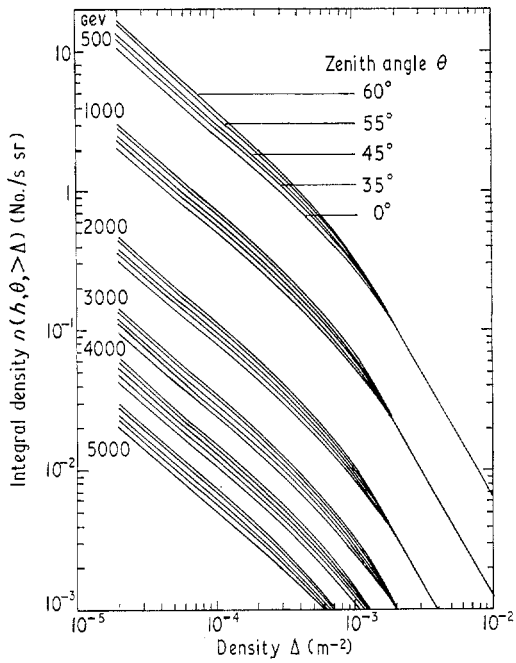

Figure 9. Empirical integral density spectrum.

Figure 9 shows the integral density spectrum for several different energies at various zenith angles as predicted by our density function using the set (*a*) parameters.

5. Summary

It is concluded from these measurements that the muon showers observed originated from the interactions of 10^{14} to 10^{15} ev isotropic cosmic ray primaries high in the atmosphere. The showers were characterized by a radial extent of 6 to 10 metres and a distribution of shower sizes M which was proportional to $M^{-\delta}$, where $3{\cdot}4 < \delta < 4{\cdot}0$. These last results are in essential agreement with the previous measurements of Barrett *et al.* (1952), who studied nearly vertical showers at comparable depths underground. Some differences are to be expected in the measurements these two experiments make, because different angular and depth ranges are covered. Both the shower radius and the distribution of shower sizes would be expected to be functions of zenith angle and depth. The exact determination of these dependencies is a topic of continuing research in the cosmic ray research group at the University of Utah.

The empirical density spectrum presented accurately predicts the energy and angular dependence, as well as the absolute rates of muon shower events, in detectors having sensitive areas of the order of 20 m^2 (the present detector) and smaller for zenith angles to 75° and depths between 1500 and 6000 hg cm^{-2}. To make empirical shower rate predictions for still larger detectors, it will be necessary to reformulate the empirical expressions in terms of a radial density distribution rather than a density spectrum, so that variations in the shower density across the detector's sensitive area can be taken into account.

References

ACHAR, C. V., *et al.*, 1965, *Proc. Phys. Soc.*, **86,** 1305–15.
BARRETT, P. H., *et al.*, 1952, *Rev. Mod. Phys.*, **24,** 133–78.
BARTON, J. C., and STOCKEL, C. T., 1968, *Can. J. Phys.*, **46,** 5318–23.
BERGESON, H. E., and WOLFSON, C. J., 1967, *Nucl. Instrum. Meth.*, **51,** 47–55.
BERGESON, H. E., *et al.*, 1967, *Phys. Rev. Lett.*, **19,** 1487–91.
BERGESON, H. E., *et al.*, 1968, *Phys. Rev. Lett.*, **21,** 1089–93.
CASTAGNOLI, G., DEMARCO, A., LONGHETTO, A., and PENENGO, P., 1965, *Nuovo Cim.*, **25,** 969–76.
CHATTERJEE, B. K., *et al.*, 1965, *Proc. 9th Int. Conf. on Cosmic Rays, London*, Vol. 2 (London: Institute of Physics and Physical Society), pp. 627–31.
CREED, D. R., *et al.*, 1965, *Proc. 9th. Int. Conf. on Cosmic Rays, London*, Vol. 2 (London: Institute of Physics and Physical Society), pp. 980–3.
HILTON, L. K., MORRIS, M. L., and STENERSON, R. O., 1967, *Nucl. Instrum. Meth.*, **51,** 43–6.
KEUFFEL, J. W., and PARKER, J. L., 1967, *Nucl. Instrum. Meth.*, **51,** 29–42.
KOBAYAKAWA, K., 1967, *Nuovo Cim.*, **47,** 156–83.
LARSON, M. O., 1968, *Ph.D. Thesis*, University of Utah.
MARTIN, E. R., 1968, *Ph.D. Thesis*, University of Utah.
MIYAKE, S., NARASIMHAM, V. S., and RAMANA MURTHY, P. V., 1964, *Nuovo Cim.*, **32,** 1505–23.
PORTER, L. G., 1968, *Ph.D. Thesis*, University of Utah.